The 33rd Computational Fluid Dynamics Symposium
Paper No. 191

A Study on Turbulent Bubbly Flows using Lattice Boltzmann Methods and Multi-phase Field Model

o Sitompul Yos, Tokyo Tech, Tokyo 152-8550, yossitompul@sim.gsic.titech.ac.jp
Takayuki Aoki, Tokyo Tech, Tokyo 152-8550, taoki@gsic.titech.ac.jp
Tomohiro Takaki, KIT, Kyoto, 606-8585, takaki@kit.ac.jp

In this study, the dynamic of turbulent bubbly flows of water-air system with high density and viscosity ratio are investigated using a direct numerical simulation. Recently, we have developed a cumulant lattice Boltzmann method for two-phase flow, which was able to simulate two-phase flows with high density ratio and Reynolds number. The method is extended by incorporating a multi-phase field model to be able to simulate the turbulent bubbly flows. The method was first validated for turbulent bubbly downflows with the reference in low density ratio settings. The turbulent bubbly downflows of water-air system was then simulated and discussed.

1. Introduction

Turbulent bubbly flows are of great importance in industrial applications, such as power plants and chemical process plants. To understand the dynamic of these flows is important for the design and operation of the plants. A direct numerical simulations have been employed in a number of studies to understand these flows, however, with low density and viscosity ratio settings due to numerical limitations [1, 2]. The present study aims to overcome these limitations and simulate a real settings of water-air system with high density and viscosity ratio.

To simulate the fluid motion, lattice Boltzmann method (LBM) is employed in this study as it is efficient for massive parallel computation [3]. LBM has been widely employed and is continually being extended for studying two-phase flows [4, 5]. Recently, we have developed a cumulant lattice Boltzmann method for two-phase flows, which was able to simulate two-phase flows with high density ratio and Reynolds number [6].

In this study, we extend our previous cumulant LBM for two-phase flows by incorporating a multi-phase field model and show that it is suited in studying the turbulent bubbly flows. Both turbulent bubbly downflows of low density ratio and water-air system has been simulated and the results are discussed herein.

2. Numerical methods

The CLBM solves the following lattice Boltzmann equations:

$$f_{ijk(x+ic\delta t)(y+jc\delta t)(z+kc\Delta t)(t+\delta t)} - f_{ijkxyzt} = \Omega_{ijkxyzt}, \quad (1)$$

where f is the discrete particle distribution function (PDF), Ω is the discrete collision operator, $\mathbf{x} = (x, y, z)$ is the position, and t is the time [7]. Eq. (1) is solved on the D3Q27 lattice which consists of 27 discrete velocities $\mathbf{e} = (e_x, e_y, e_z)$, where $i = e_x/c$, $j = e_y/c$, $k = e_z/c$, $i, j, k \in \{\bar{1}, 0, 1\}$ (Miller indices with $\bar{1} \equiv -1$ is used), $c = \delta x/\delta t$ is the lattice speed, δx is the lattice spacing, and δt is the lattice time step.

Eq. (1) is split it into collision and streaming steps as follows:

$$f^*_{ijkxyzt} = f_{ijkxyzt} + \Omega_{ijkxyzt}, \quad (2)$$

$$f_{(x+ic\delta t)(y+jc\delta t)(z+kc\Delta t)(t+\delta t)} = f^*_{ijkxyzt}, \quad (3)$$

where f^* is the post-collision PDFs. The collision step of Eq. (2) is then solved in cumulant space as follows:

$$c^*_{\alpha\beta\gamma} = c_{\alpha\beta\gamma} - \omega_{\alpha\beta\gamma}\left(c_{\alpha\beta\gamma} - c^{eq}_{\alpha\beta\gamma}\right), \quad (4)$$

where c denotes cumulants, $\alpha, \beta, \gamma \in \{0,1,2\}$ are the order of the cumulants, and ω is the relaxation rates. The cumulants can be obtained from the distribution function using the following transformation:

$$c_{\alpha\beta\gamma} = c^{-(\alpha+\beta+\gamma)} \frac{\partial^{\alpha+\beta+\gamma}}{\partial \Xi_x{}^{\alpha} \partial \Xi_y{}^{\beta} \partial \Xi_z{}^{\gamma}} ln\left(\mathcal{L}\left[f(\underline{\xi})\right]\left(\underline{\Xi}\right)\right)\Big|_{\underline{\Xi}=0}, \quad (5)$$

where $\mathcal{L}$ is the Laplace transformation.

The cumulant collision model is employed within a velocity-based formulation of two-phase LBM where the zeroth order moment is set as to unity. Without any corrections, the formulation will recover the following pressure-less momentum equations:

$$\frac{\partial \mathbf{u}}{\partial t} + \mathbf{u} \cdot \nabla \mathbf{u} = \nabla \cdot [\nu(\nabla \mathbf{u} + \nabla^{\mathrm{T}} \mathbf{u})]. \quad (6)$$

To obtain correct momentum equations, several terms are added as external forces:

$$\mathbf{F} = \mathbf{F}^p + \mathbf{F}^\nu + \mathbf{F}^b + \mathbf{F}^s, \quad (7)$$

$$\mathbf{F}^p = -\nabla p, \quad (8)$$

$$\mathbf{F}^\nu = \nu[\nabla \mathbf{u} + (\nabla \mathbf{u})^T] \cdot \nabla \rho, \quad (9)$$

$$\mathbf{F}^b = \rho \mathbf{g}, \quad (10)$$

$$\mathbf{F}^s = -\sigma(\nabla \cdot \mathbf{n})\nabla \phi, \quad (11)$$

where $\mathbf{F}^p$, $\mathbf{F}^\nu$, $\mathbf{F}^b$, and $\mathbf{F}^s$ are the pressure, viscous, body, and surface forces, respectively; $\mathbf{g}$ is the gravity acceleration and σ is the surface tension. The kinematic viscosity ν is related to the following hydrodynamic relaxation rate:

$$\omega_h = \left(\frac{3\nu\delta t}{\delta_x^2} + \frac{1}{2}\right)^{-1}. \quad (12)$$

The relaxation rates other than ω_h are set to unity in this study.

We updated the pressure and momentum iteratively for each time step as follows:

$$p^{*,i+1} = p^i + \rho c_s^2 \nabla \cdot \mathbf{u}^{*,i} + \frac{\alpha}{N} \nabla^2 p^i, \quad (13)$$

$$\mathbf{u}^{*,i+1} = \sum_\alpha \mathbf{e}_\alpha f_\alpha + \frac{1}{2} \mathbf{F}^{*,\boldsymbol{i+1}} \delta t, \quad (14)$$

where the superscript i indicates the current iteration step, N is the number of iterations, and α is the diffusivity of the Laplacian of

Copyright © 2019 by JSFM

pressure. After the iterations finish (currently five iterations), the pressure and velocity at the advanced time step are set as:

$$p^{n+1} = p^{*,N}, \tag{15}$$

$$\mathbf{u}^{n+1} = \mathbf{u}^{*,N}. \tag{16}$$

To satisfy the incompressible flow condition, the Mach number should be kept low:

$$Ma = \frac{|\mathbf{u}|}{c_s} \ll 1. \tag{17}$$

To capture the interface dynamics for many bubbles without numerical bubble coalescing, the following multi-phase-field model is employed:

$$\frac{\partial \phi_i}{\partial \mathrm{t}} + \nabla \cdot (\phi_i \mathbf{u}) = M\left[\nabla \cdot \left\{\nabla \phi_i - \frac{\phi_i(1-\phi_i)\boldsymbol{n}_i}{W}\right\}\right] - \frac{{\phi_i}^2}{\sum_{j=1}^{N} {\phi_j}^2} \sum_{j=1}^{N}\left[\nabla \cdot \left\{\nabla \phi_j - \frac{\phi_j(1-\phi_j)\mathbf{n}_\mathrm{j}}{W}\right\}\right], \tag{18}$$

where ϕ is the phase-field variables, M is the mobility, W is the interface half-width, and $\mathbf{n}$ is the interface normal vector [8]. The superscript i indicates the current phase and N is the number of phases.

The model is solved using finite volume method where a third-order weighted essentially non-oscillatory (WENO) scheme is used to discretize the advection term and a third-order TVD Runge-Kutta method is used for time integration. The density and viscosity are calculated as follows:

$$\rho = \phi_d \rho_l + (1-\phi_d)\rho_h, \tag{19}$$

$$\upsilon = \phi_d \upsilon_l + (1-\phi_d)\upsilon_h, \tag{20}$$

$$\phi_d = \sum_{i=1}^{D} \phi_i, \tag{21}$$

where subscript d indicates the dispersed phase (bubbles) and superscript D indicates the number of dispersed phases (number of bubbles).

3. Results and Discussions

Turbulent bubbly downflows which appears in advanced nuclear power reactors are considered in this study. A vertical channel with size of $\pi \times 2 \times \pi/2$ are examined where the streamwise, wall-normal, and spanwise direction are denoted by *x*, *y*, and *z* direction, respectively. The flow is driven by a constant pressure gradient and gravity in negative *x* direction. Periodic boundary conditions are applied to the streamwise and spanwise direction. No slip conditions are applied at the walls [1].

Two cases are simulated: a system with density ratio of 10 and a water-air system. The parameters for both cases are shown in Table 1 in SI unit. The Eotvos and Morton number are defined as:

$$Eo = \frac{\rho_h g D^2}{\sigma}, \tag{22}$$

$$Mo = \frac{g \mu_h^4}{\rho_h \sigma^3}. \tag{23}$$

The Morton number is material properties and the value for water-air system is 2.55×10^{-11}. Therefore for the same Eotvos number with the reference problem with density ratio of 10, the bubble diameter is determined to be 1.52×10^{-3}. The sum of pressure gradient and the weight of the mixture is constant and determined using:

$$\tau_w = \left(\frac{dp}{dx} + \rho_{avg} g\right) H = \beta H, \tag{24}$$

where τ_w is the wall shear stress, ρ_{avg} is the average density of the mixture, H is the half-width, and β is the sum of pressure gradient and the weight of the mixture. The void fraction of 1.5% are examined in this study.

Table 1. Simulation parameters (SI unit)

Parameters	Density ratio = 10	Water-air
Eo	3.13E-01	3.13E-01
Mo	1.54E-10	2.55E-11
ρ_h	998	998
μ_h	1.00E-03	1.00E-03
g	9.8	9.8
ρ_l	99.8	1.2
μ_l	1.00E-03	1.80E-05
σ	4.00E-02	7.28E-02
D	1.13E-03	1.52E-03

The turbulent pressure and velocity fields for the single phase flow are used as initial conditions. Bubble are then put in the channel with regular configuration of 3 × 3 × 2 bubbles and let to develop for non-dimensional period of $t^* = 150$, where the time is non-dimensionalized by half-width and average mean velocity of single-phase flow. The turbulent statistics are then calculated for the following period of $t^* = 150$. The results of the present simulation are shown in the following two sub-sections.

3.1. Turbulent bubbly downflows with low density ratio

The bubble distribution for void fraction 1.5% the final time.is shown in Fig. 1. The bubble shapes between the present and reference (1) are relatively very close. The bubble tends to gathered in the center of the flow to balance the shear stress, pressure gradient, and weight of the mixture. Similar with the reference much vorticity appear behind the bubbles as the buoyancy of the bubbles against the downlow.

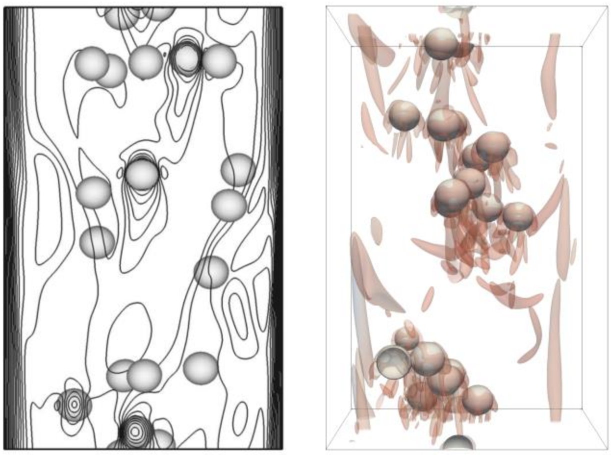

Fig. 1 The bubble distribution for void fraction of 1.5%. (left) Lu and Tryggvason (right) present simulation.

The void fraction and streamwise mean velocity are shown in Figs. 2 and 3, respectively. There are some differences with the reference, where more bubbles are suggested to gather in the center by the references. However, the general behavior are quite similar where bubbles gathered at the center and the maximum streamwise velocity are suppressed by the existence of bubbles.

Copyright © 2019 by JSFM

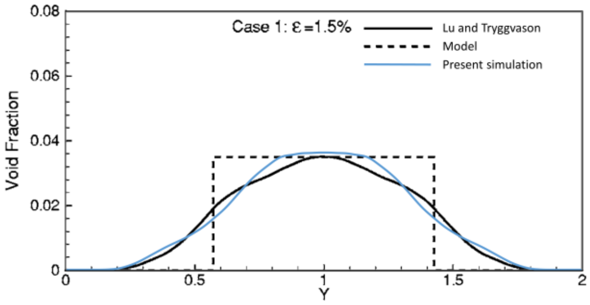

Fig. 2 Void fraction distribution for void fraction of 1.5%. (black) Lu and Tryggvason, (blue) present simulation.

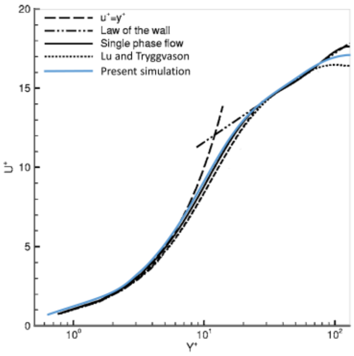

Fig. 3 Streamwise mean velocity distribution for void fraction of 1.5%. (black) Lu and Tryggvason, (blue) present simulation.

3.2. Turbulent bubbly downflows with high density ratio

The turbulent downflows for water-air system has been simulated stably. In this case, the bubble are more deformed, showing ellipsoidal shape. Because the bubble are more deformed they easily move in the channel. Fig. 4 shows the bubble distribution at the final time for void fraction 1.5%. In this case, the bubbles are distributed more homogeneously in the channel. More vortices appears in entire channel.

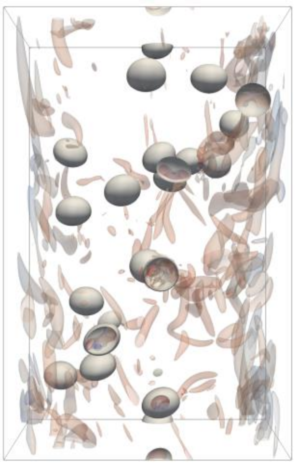

Fig. 4 The bubble distribution for water-air system with void fraction of 1.5%

Figs. 5 and 6 show the void fraction and streamwise mean velocity distribution of the water-air system in comparison with low density ratio case. The void fraction and streamwise velocity are quite different from the low density ratio case where bubbles are more dispersed and the mean velocity is suppressed more homogeneously. It seems that the bubbles affect the turbulent flow more in the case of water-air system. This results, however, need to be further studied by calculating other turbulent statistics.

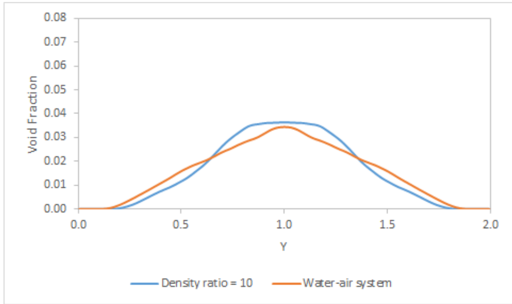

Fig. 5 Comparison of void fraction distribution. (blue) density ratio of 10, (orange) water-air system.

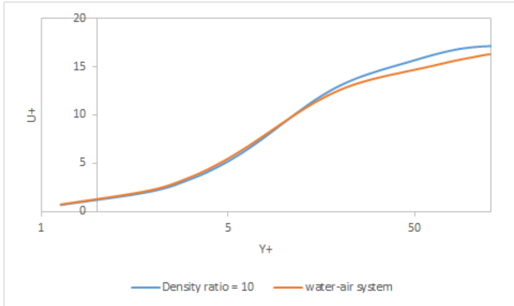

Fig. 6 Comparison of streamwise mean velocity distribution. (blue) density ratio of 10, (orange) water-air system.

4. Conclusions

A cumulant lattice Boltzmann method with multi-phase model has been developed for simulating turbulent bubbly channel flow with high density and viscosity ratio. First, the turbulent bubbly downflows with low density ratio were simulated and compared with the reference. The results show the general behavior of the obtained flow are the same with the reference where the bubbles tends to fill the center of the channel and suppressed the mean velocity at the center. Much vortices appear behind of the bubbles in this case. Finally, the turbulent bubbly downflows for water-air system is simulated. The results show that the bubbles are more deformed and dispersed. More vortices appear in this case than in the low density ratio case. The mean velocity is suppressed more homogeneously. This result show that using the assumption of low density ratio for simulating water-air system may not be correct.

Bibliography

(1) Lu, J. and Tryggvason. G., "Numerical study of turbulent bubbly downflows in a vertical channel," *Physics of Fluids* 18.10, pp. 103302 (2006).

(2) Cifani, P., Kuerten, J. G., and Geurts, B. J., “Highly scalable DNS solver for turbulent bubble-laden channel flow,” *Computers & Fluids*, 172, pp. 67-83 (2018).

(3) Sterling, J. D. and Chen. S., "Stability Analysis of Lattice Boltzmann Methods," *Journal of Computational Physics* 123.1, pp. 196-206 (1996).

Copyright © 2019 by JSFM

(4) Fakhari, A., Geier M. and Lee T. "A Mass-Conserving Lattice Boltzmann Method with Dynamic Grid Refinement for Immiscible Two-Phase Flows," *Journal of Computational Physics* 315, pp. 434-457 (2016).

(5) Inamuro, T., *et al*. "An Improved Lattice Boltzmann Method for Incompressible Two-Phase Flows with Large Density Differences," *Computers & Fluids* 137, pp. 55-69 (2016).

(6) Sitompul, Y. P., and Aoki, T., “A filtered cumulant lattice Boltzmann method for violent two-phase flows,” *Journal of Computational Physics*, 390, pp. 93-120 (2019).

(7) Geier, M., *et al*. "The Cumulant Lattice Boltzmann Equation in Three Dimensions: Theory and Validation," *Computers & Mathematics with Applications* 70.4, pp. 507-547 (2015).

(8) Geier, M., Fakhari, A. and Lee, T. "Conservative Phase-Field Lattice Boltzmann Model for Interface Tracking Equation," *Physical Review E* 91.6, pp. 063309 (2015).

(9) Aihara, S., Takaki, T., and Takada, N., “Multi-phase-field modeling using a conservative Allen–Cahn equation for multiphase flow,” *Computers & Fluids*, 178, pp. 141-151 (2019).

Copyright © 2019 by JSFM